Título artículo / Títol article:	Ultrafast characterization of the electron injection from CdSe quantum dots and dye N719 co-sensitizers into TiO2 using sulfide based ionic liquid for enhanced long term stability
Autores / Autors	Victoria González Pedro, Qing Shen, Vasko Jovanovskid, Sixto Giménez Juliá, Ramón Tena-Zaera, Taro Toyoda, Iván Mora Seró
Revista:	Electrochimica Acta, 2013, vol. 100
Versión / Versió:	Pre-print
Cita bibliográfica / Cita bibliogràfica (ISO 690):	González Pedro, Victoria ; Shen, Qing ; Jovanovskid, Vasko ; Giménez Juliá, Sixto ; Tena-Zaera, Ramón ; Toyoda, Taro ; Mora Seró, Iván *Electrochimica Acta*, 2013, vol. 100, p. 35–43
url Repositori UJI:	http://hdl.handle.net/10234/91501

Ultrafast Characterization of the Electron Injection from CdSe Quantum Dots and Dye N719 Co-sensitizers into TiO_2 Using Sulfide Based Ionic Liquid for Enhanced Long Term Stability

Victoria González-Pedro,[1] Qing Shen,[2, 3,*] Vasko Jovanovski[4,5], Sixto Giménez,[1] Ramon Tena-Zaera,[5] Taro Toyoda[2] and Iván Mora-Seró[1,*]

[1] Photovoltaics and Optoelectronic Devices Group, Departament de Física, Universitat Jaume I, 12071 Castelló, Spain.

[2] Department of Engineering Science, Faculty of Informatics and Engineering, The University of Electro-Communications, 1-5-1 Chofugaoka, Chofu, Tokyo 182-8585, Japan.

[3] PRESTO, Japan Science and Technology Agency (JST), 4-1-8 Honcho, Kawaguchi, Saitama 332-0012, Japan.

[4] Energy Department, IK4-CIDETEC, Parque Tecnológico, Paseo Miramón 196, Donostia-San Sebastián, 20009, Spain.

[5] Analytical Chemistry Laboratory, National Institute of Chemistry, Hajdrihova 19, SI-1000 Ljubljana, Slovenia.

Email: shen@pc.uec.ac.jp, sero@uji.es

2 May 2014

Abstract

Combination of inorganic Quantum Dots (QDs) and organic/metallorganic dyes as supracollectors nanocomposites could have an important role on the development of efficient photovoltaic devices based on the synergistic action of the hybrid-sensitizers. Here we have analyzed the combination of CdSe QDs and polypyridil N719 ruthenium dye. By ultrafast transient grating measurements we show that the cascading structure

(type II) of this system takes full advantage to augment electron injection and hole regeneration efficiencies. Co-sensitized TiO_2 electrodes lead to an improvement in charge separation, increasing the number of injected electrons from the CdSe QDs to the TiO_2 as a consequence of the suppression of back reaction, by fast regeneration of holes by the dye action. The potentiality of this supracollector system has been verified in a complete cell configuration. Sulfide/polysulfide based ionic liquid in which both sensitizers (QD and dye) are stable has been employed as hole conducting media. In spite of the limited efficiencies of the analyzed cells, the higher photocurrents measured for CdSe/N719 co-sensitization compared to the cells sensitized using a single sensitizer constitutes a valid proof of the concept. Impedance spectroscopy unveiled the recombination limitation of the analyzed cells. On the other hand, ionic liquid exhibits an enhanced cell stability maintaining cell efficiency after one week and keeping it at 80% after 21 days. The reported results highlight a huge potential of the synergetic combination of QD and dyes for improving solar cell performance and of novel sulfide/polysulfide ionic liquid-based electrolytes for enhancing long term stability and sustainability of QD sensitizers.

Introduction

The increasing worldwide demand for clean energy and the limited fossil fuels reserves on the planet require development of reliable and renewable energy sources. Among the various technologies available nowadays Quantum Dot Sensitized Solar Cells (QDSCs) have attracted a great deal of attention due to its extremely easy fabrication, and relatively low production cost.[1-4] Furthermore, the use of semiconductors as sensitizers has some unique advantages as the high extinction coefficients due to the quantum confinement, tunable band gap from the infra-red to the ultraviolet by adjusting the size,[5] large intrinsic dipole moments which may lead to a rapid charge separation, and the possibility of multiple electron generation (MEG)[6, 7] which gives to QDSCs the capability to achieve quantum yields, or even external quantum efficiency, greater than 100%.[8, 9]

In addition, semiconductor QDs are excellent building blocks for the design of light supracollecting structures by the synergetic combination of different types of QDs,[10, 11] or QDs and dyes.[12-20] Different QDs and dye hybrid systems have been explored with

the aim to exploit their interacting proprieties. In this heterostructures, performance can arise from the fast scavenging of photogenerated holes in quantum dots by a molecular dye. This process can outbalance the competition between the electron transfer into the TiO_2 and the internal relaxation of the quantum dot excited state, leading to a better charge separation and higher electron injection yields.[15, 19] Simultaneously, the combined use of QD and dye enhances the light harvesting wavelength range due to the combined absorption of the two assembled sensitizers.[12, 17, 18]

Although hybrid sensitized systems appear promising, only few examples have been reported showing clear synergistic effects due to the lack of an appropriate electrolyte, compatible with all individual chromophores. The well established I^-/I_3^- electrolyte cannot be used with quantum dot sensitizers due to the highly corrosive nature of the polyiodide species with most of the semiconductors.[1, 21, 22] On the other hand, the common electrolyte for chalcogenide QDSCs in liquid devices, polysulfide aqueous electrolyte,[23] promotes the dye detachment from TiO_2 surface due to its high pH value (~ 13). Therefore, different redox couples such as iron (II/III)[24] and cobalt (II/III)[25] complex-based electrolytes with the ability of regenerating oxidized forms of QDs and dyes have been proposed as alternative systems. Besides, the use of TiO_2[17] or Al_2O_3[18] coatings has also been explored as alternative to protect one of the two light absorbing materials. Most recently, solvent-free ionic liquid based electrolytes containing sulfide/polysulfide redox couple compatible with inorganic sensitizers have been reported, being a promising alternative for this type of efficient supracollector nanocomposites, and adding the advantages of ionic liquid electrolytes, such as, non-volatility, non-flammability and high ionic conductivity, among others.[26]

We have studied, in precedent works, the charge separation in hybrid sensitized electrodes with surface photovoltage[15, 19] (SPV) and photoluminescence[16] (PL). These studies are completed in this work. Here, we make a global approach to the synergistic interaction of QDs and dyes. We have studied the ultrafast injection of carriers with and without electrolyte in the ps timescale. These new data complements the recombination characterization, in the μs timescale, carried out previously.[16] On the other hand, QDSCs have been prepared using electrodes sensitized in the same way and sulfide/polysulfide-based Ionic Liquid (IL) electrolyte. The potentiality of QDs and dye supracollectors systems is demonstrated by higher photocurrent, J_{sc}, compared to the

single sensitizers. We also report, up to our best knowledge, the first results for a QD/dye hybrid sensitized systems working with an ionic liquid electrolyte in a regenerative cell showing the capability of this type of electrolytes for regenerating the oxidized form of both QDs and dyes, whereas other electrolytes work well only with one sensitizer. The cells exhibit no decrease in efficiency after one week and maintain 80% of the original performance after 21 days. In addition, a high recombination rate, especially with dye sensitization, has been identified limiting the final cell efficiency.

Experimental Section

Preparation of co-sensitized TiO_2-CdSe-N719 nanoporous electrodes. A double TiO_2 layer configuration was employed as working electrode. On a FTO conducting glass (Pilkington TEC15, ~15Ω/sq resistance) a 8 μm-thick transparent layer (Dyesol, 18NR-T, 20 nm average particle size) was first screen-printed and then coated by a 4 μm-thick second layer of scattering titania particles (Dyesol, WERO-4, 300-400 nm particle size distribution).The resulting photoelectrodes were sintered at 450º C for 30 min to obtain a good electrical contact between the nanoparticles. The SnO_2:F (FTO) coated glass was previously covered by a compact layer of TiO_2 deposited by spray pyrolisis (thickness ~150 nm).

For the time-resolved measurements nanocrystalline transparent TiO_2 thin films were prepared by using a method reported by Shen et al.[27, 28] In this case, a TiO_2 paste was prepared by mixing 15 nm nanoparticles (SuperTitania, Showa Denko; anatase structure) and poly(ethylene glycol) (PEG) in pure water. After deposition onto FTO glass, the TiO_2 film was sintered in air at 450 °C for 30 min. The thickness of the film was 11 μm.

The mesoporous TiO_2 electrodes were sensitized *in-situ* by CdSe QDs grown by Succesive Ionic Layer Adsorption and Reaction (SILAR). For this purpose, two solutions of 0.03 M $Cd(NO_3)_2$ dissolved in ethanol and another one containing the *in situ* generated 0.03 M selenide (Se^{2-}) in ethanol were used.[29, 30] A single SILAR cycle consisted of 30 seconds dip-coating of the TiO_2 working electrode into the metal precursor (Cd^{2+}) and subsequently into the selenide solution, also during 30 seconds . The SILAR was carried out inside a glove box under N_2 atmosphere. After each

precursor bath the photoanode was thoroughly rinsed by immersion in ethanol in order to remove the chemical residues from the surface and then dried with a N_2 gun. This procedure was repeated seven times. For dye sensitization a squared TiO_2 electrode (~0.25 cm^2) was stained by immersing it into a N719 dye solution 0.3 M in a mixture of acetonitrile and tert-butanol (v/v=1/1) for 16 h. The same procedure was used for co-sensitization but using electrodes previously sensitized with CdSe. At least two samples were prepared with each kind of sensitization.

Preparation of sulfide/polysulfide ionic liquid-based electrolytes. Firstly, 1-butyl-3-methylimidazolium sulfide ionic liquid was synthesized following the procedure reported elsewhere[26,31]. In brief, 28 mmol of 1-butyl-3-methylimidazolium chloride (Solvionic) and 7.5 g (31 mmol) of $Na_2S{\cdot}9H_2O$ were dissolved in 50 ml of methanol at 50 °C. A white precipitate (NaCl) formed immediately. Methanol and water were removed *in vacuo* and more dry methanol was added in order to remove traces of water. This procedure was repeated several times keeping the solution at low temperatures, i.e. ~ -20 ºC in between each step and finally adding acetonitrile to remove last traces of NaCl and Na_2S by filtration followed by *in vacuo* removal of the solvent in order to purify the final product.

Secondly, an equimolar amount of molecular sulfur was dissolved in the 1-butyl-3-methylimidazolium sulfide ionic liquid, leading to formation of the ionic liquid 1-butyl-1-methylimidazolium S^{2-}/S_n^{2-} redox couple.

Finally, the electrolyte was prepared by mixing 1-butyl-3-methylimidazolium sulfide/polysulfide ionic liquid and a valeronitrile:acetonitrile mixture (v/v=1:1) in 1:2 weight/volume ratio.[26]

Electrode and cell characterization. The Incident Photon to Current Efficiency (IPCE) measurements were performed by employing a 150 W Xe lamp coupled with a computer controlled monochromator, photocurrent was measured by using an optical amperimeter 70310 from Oriel Instruments using a Si photodiode to calibrate the system. Current-Potential (J-V) curves and impedance spectroscopy (IS) measurements were obtained using a FRA equipped PGSTAT-30 from Autolab. The cells were illuminated using a solar simulator at AM 1.5 G, where the light intensity was adjusted with an NREL-calibrated Si solar cell with a KG-5 filter to 1 sun intensity (100 $mWcm^-$

^{2}). Impedance spectroscopy (IS) measurements were carried out in dark conditions at forward bias, applying a 20 mV AC sinusoidal signal over the constant applied bias with the frequency ranging between 400 kHz and 0.1 Hz. Measurements were carried out using mask and without antireflective layer.

Ultrafast carrier dynamics. The principle and setup of the lens-free heterodyne detection transient grating (LF-HD-TG) technique have been reported in detail in previous papers.[27, 32-37] In this experiment, the laser source was a titanium/sapphire laser (CPA-2010, Clark-MXR Inc.) with a wavelength of 775 nm, a repetition rate of 1 kHz, and a pulse width of 150 fs. The light beam was split into two parts. Half of it was used as a probe pulse. The other half of the light was used to pump an optical parametric amplifier (OPA) (a TOAPS from Quantronix) to generate light pulses with a wavelength tunable from 290 nm to 3 μm. It was used as a pump light in the TG measurement. In this study, the pump pulse wavelength was 520 nm and the probe pulse wavelength was 775 nm. At least two samples prepared at each analyzed condition have been characterized with LF-HD-TG, obtaining a good agreement in the TG pattern among samples prepared in the same way. This fact indicates the reproducibility of measurements reported in Fig. 1.

Cell fabrication. The devices were assembled with a counter electrode (thermally platinized TCO), using a Surlyn© (Dupont) thermoplastic frame (25 μm thick). Redox IL electrolyte (1-butyl-3-methylimidazolium sulfide:sulfur; molar ratio=1:1) diluted ((w/v)=1:2) in valeronitrile:acetonitrile mixture (v/v=1:1) was introduced through a hole drilled in the counter electrode that was sealed afterwards.

Results and Discussion

In order to study the interaction between QDs and dyes we have studied probably the most popular sensitizers for QDSCs and dye sensitized solar cells: CdSe QDs and N719, respectively. These materials present a favorable type II alignment (cascade structure) which promotes the electron injection and hole extraction efficiencies.[15, 16] Electrodes coated with a single sensitizer (CdSe or N719) and with both sensitizers (first CdSe and N719 over it) have been analyzed.

These electrodes were examined first by ultrafast carrier dynamics to reveal factors

concerning the injection process. Fig. 1(a) shows the transient grating (TG) response of the CdSe QDs adsorbed on TiO_2 measured in air and in ionic liquid. The experiment was carried out with pump pulse wavelength of 520 nm and the probe pulse wavelength of 775 nm. Upon this excitation wavelength the optical absorption of the anatase TiO_2 electrode is negligible and the TG signals can be considered to result from the optical absorption of the CdSe QDs and the dye.[27, 35] The TG signal of the semiconductor QDs on the fast time scale used in this study (less than 1 ns) is proportional to the change in the refractive index $\Delta n(t)$ of the sample due to photoexcitation, which can be approximately determined by[35, 38-41]

$$\Delta n(t) = A\left(\frac{N_e(t)}{m_e} + \frac{N_h(t)}{m_h}\right) \quad (1)$$

where the first and second terms are the changes in refractive index induced by photoexcited electrons and holes, respectively. $N_e(t)$ and $N_h(t)$ are the photoexcited electron and hole densities, respectively. m_e and m_h are the effective masses of electrons and holes, respectively. A is a constant. The important feature is that both the photoexcited electron and hole carrier densities in the QDs contribute to the TG signal. In principle, the exact contribution to $\Delta n(t)$ by electrons and holes depends inversely on their effective mass. According to the Drude theory,[38, 41] we can consider that only free photoexcited electrons and holes are responsible for the population grating signals.[35, 39, 40] For bulk CdSe, the effective masses of electrons and holes are $0.13m_0$ and $0.44m_0$ (m_0 is the electron rest mass), respectively,[42] so both the photoexcited electron and hole carrier densities in the CdSe QDs contribute to the signal. It is known that the effective mass of electrons for TiO_2 is about 30 m_0, which is about two orders of magnitude larger than in the case of CdSe. Therefore, the TG signal due to the injected electrons in TiO_2 can be ignored.[35, 40]

We found that the TG response for CdSe sensitized electrode can be fitted very well with a double exponential decay plus an offset, as shown in Eq. (2),

$$TG = A_1 e^{-t/\tau_1} + A_2 e^{-t/\tau_2} + A_3 \quad (2)$$

where A_1, A_2 and A_3 are constants, and τ_1 and τ_2 are the time constants of two decay processes. Here, the constant term A_3 corresponds to the slowest decay process, in which the decay time (in the order of ns) is much larger than the time scale of 400 ps measured

in this study. The three different decay processes have a weight in the total decay process defined as $A_i/(A_1+A_2+A_3)$, where i=1, 2 and 3 is the process that is weighted.

We measured the dependence of the TG responses on the pump intensity and found that the dependence of the maximum signal intensity on the pump intensity was linear, and that the waveforms of the responses overlapped each other very well when they were normalized. These results mean that the time constants were independent of the pump intensity, and many-body recombination processes such as Auger recombination could be neglected. Therefore, it is reasonable to assume that the decay processes of photoexcited electrons and holes in the CdSe QDs are due to one-body recombination processes, such as, trapping and transfer. As a preliminary hypothesis each decay time could be assigned to one kind of carriers, electrons or holes. However, by taking into account the effective masses of electrons and holes in CdSe, the amplitude coefficients (A_1 and A_2) need to keep a 1-fourth relation as the effective masses, see Table 1, this hypothesis is not feasible. In light of this effect, the participation of electrons in first exponential decay cannot be neglected and as discussed in previous works for cadmium chalcogenides, the fast decay, A_1, can be attributed to electron injection from CdSe QDs in direct contact with TiO_2 with contribution of hole trapping.[33, 43] The slow decay, A_2, involves electron injection from QDs not in direct contact with the TiO_2 which are transferred to TiO_2 through CdSe interfaces and electron trapping.[1, 33, 34, 44] Finally the slowest decay process, A_3, (not analyzed in this work) is related with the recombination processes. The correlation between the different decays and the physical processes originating them have been also investigated in a previous work[33] comparing the TG response of CdSe on TiO_2 and on glass, where no photoinjection is produced.

Next, to separate the photoexcited electron and hole dynamics that contribute to the TG response, we measured the TG responses of the same sample in air and in IL. As shown in Fig. 1(a), a clear difference can be observed between these two TG responses for CdSe sensitized electrodes. By normalizing the two TG responses at the signal intensity of 400 ps, we found that they overlapped with each other very well for time periods longer than 200 ps. The time constants of the fast (τ_1) and slow (τ_2) decay processes of photoexcited carriers for CdSe sensitized electrode in air and IL are not significantly different, only a slower second component is observed with IL, see Table 1. Thus, the difference observed can be ascribed to a quenching of the signal coming

from the decays A_1 and A_2 in the IL electrolyte, obtaining a lower signal at the resolution time of the setup (~0.2 fs), see Fig. 1(a). The weight of the two fastest decays to the total decay process is lower when the CdSe sensitized electrode is in contact with the IL, see Table 1. This difference can be explained as an ultrafast hole trapping/transfer in presence of IL. Therefore, the "apparent disappearance" of the fastest decay processes in the IL electrolyte implies that the hole trapping/transfer to the S^{2-} ions, which are supposed to be strongly adsorbed onto the CdSe QD surface, can be too fast in these circumstances as indicated by Hodes[1] and therefore could not be observed under the temporal resolution (about 200 fs) of our TG technique. This result is analogous to the previously observed for CdSe electrodes in aqueous Na_2S solution.[45] This observation is particularly important, as the result suggests that the trapping/transfer of holes in QDs, with diameters of a few nm, to sulfur hole acceptors strongly adsorbed on the QD surface[1] could approach a few hundreds of fs.[46]

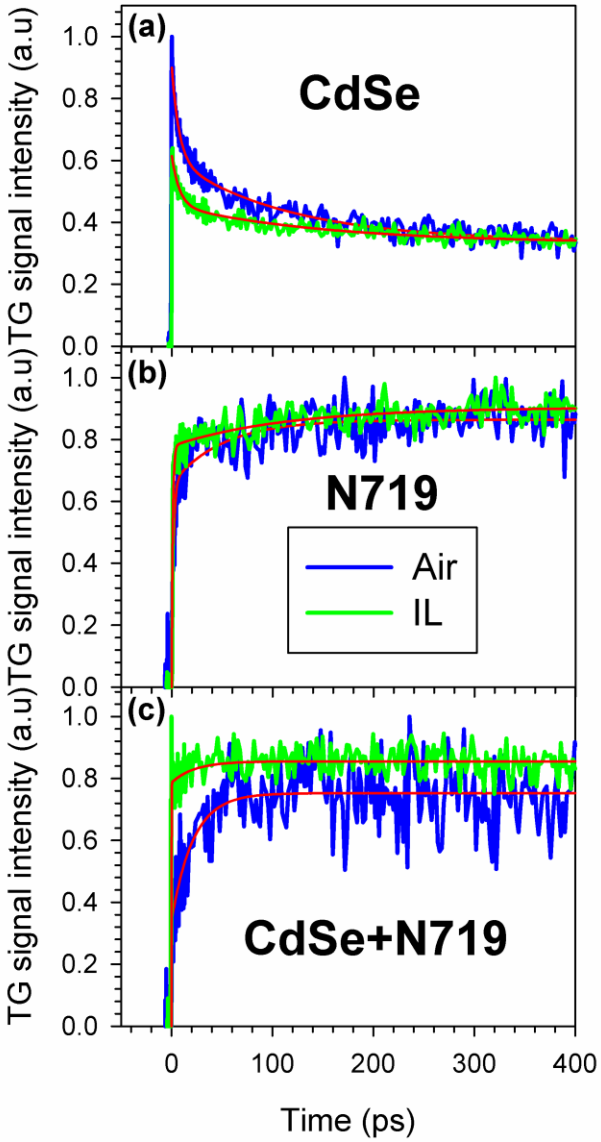

FIG. 1. TG responses of TiO_2 nanostructured film sensitized with a) CdSe; b) N719 and c) CdSe-N719. Measured with the electrodes in air an in the ionic liquid electrolyte.

Fig. 1(b) shows the TG response of the N719 adsorbed on TiO_2 measured in air and in IL. In the case of N719 dye adsorbed on TiO_2 the pattern observed is significantly different than in CdSe sensitized electrode, see Fig. 1. In the case of N719 dye the TG response has been identified with the photogeneration of N719 cations (oxidized state of N719) by photoexcitation and subsequent electron injection into TiO_2.[47] The fast rise of the TG signal shown in Fig. 1(b) correspond to the electron injection processes from the

excited states of N719 to the conduction band (CB) of TiO_2. The generation of oxidized dye is multiexponential and can be well fitted to two components as follows:[38, 47]

$$TG = A_1\left(1 - e^{-\frac{t}{t1}}\right) + A_2\left(1 - e^{-\frac{t}{t2}}\right) \qquad (3)$$

where τ_1 and τ_2 are time constants, and A_1 and A_2 are the contributions from the two components. The time constants τ_1 and τ_2 of the dye sensitized electrode on air corresponding to two electron injection processes were 1.7 ps ($A_1/(A_1+A_2)$: 76%) and 50 ps ($A_2/(A_1+A_2)$: 24%), respectively. There are two possible explanations for the origin of the two processes. The first one is that the two injection dynamics can be considered to be biphasic. In this case, the 1.7 ps ultrafast component resulted from the singlet excited state; the metal-to-ligand charge-transfer (^{1}MLCT) and the 50 ps slower component originated from the triplet excited state (^{3}MLCT).[48, 49] It has been reported that the electron injection rate from the singlet excited state of N719 to metal oxide electrodes is one order of magnitude faster than that from the triplet state. [38, 46] Another explanation could be that both the two injection processes mostly correspond to electron injection processes from the triplet excited state due to some inhomogeneities in the TiO_2 nanoparticle surfaces, resulting in different electronic couplings between N719 and the TiO_2. Considering the ultrafast intersystem crossing time of 100 fs from the singlet excited state to the triplet excited state in N719, the electron injection from the singlet excited state would be unfavorable if the injection time was longer than 100 fs and its component would be small.[48] The component of the fast injection process measured here is as large as 76%, suggesting that the latter explanation is more reasonable.[47-49] As shown in Fig. 1(b), the TG response of N719 on TiO_2 measured in IL showed no qualitative change with respect to the electrode in air, see Fig. 1(b). Only, some difference in τ_2 could be found in the N719 sensitized electrode in IL, see Table 1.

Table 1. Fitting parameters of TG responses according Eq. 2 for CdSe sensitized sample and Eq. 3 for N719 and CdSe/N719 sensitized samples. The weight of each decay (growth) has been obtained using the formula $A_i/(A_1+A_2+A_3)$ ($A_i/(A_1+A_2)$) for the CdSe sample (N719 and CdSe/N719 samples), where i=1, 2 and 3 is the process that is weighted

Sample	τ_1 **(ps)**	τ_2 **(ps)**	A_1	A_2	A_3	**Weight** A_1	**Weight** A_2	**Weight** A_3
CdSe air	7±1	114±6	0.3	0.27	0.34	33%	30%	37%

CdSe IL	7±1	150±12	0.16	0.12	0.33	26%	20%	54%
N719 air	1.7±0.2	50±9	0.66	0.21	-	76%	24%	-
N719 IL	1.1±0.1	114±26	0.78	0.12	-	87%	13%	-
CdSe/N719 air	0.2	22±3	0.40	0.48	-	45%	55%	-
CdSe/N719 IL	0.2	18±6	0.82	0.09	-	90%	10%	-

Fig. 1(c) shows the TG response of the CdSe/N719 sensitized TiO_2 measured in air and in IL. The TG response pattern was very similar to those of N719 on TiO_2, which indicates that TG signal reflect the production of N719 cations. By fitting with Eq. (3), the time constants τ_1 and τ_2 of the two electron injection processes in air were 0.2 ps (the resolution limit of the experimental set up) and 21 ps, respectively, see Table 1. The two decay times were much smaller than those of only N719 adsorbed on TiO_2. The increase of the TG signal in the case of N719 on TiO_2 at the fast time scales of a few ps and a few tens of ps is due to the production of N719 cation, i.e. the electron injection from N719 to TiO_2.[47] Similarly, in the case of CdSe/N719, we can consider the increase of the TG signals resulted from the production of oxidized N719. The N719 cation can be produced by the electron injection from N719 to TiO_2 and to CdSe, and also by hole transfer from CdSe to N719 as shown in Fig. 2. This fact points to the fast charge separation due to the co-sensitization of both N719 and CdSe QDs (type II). The TG response of CdSe/N719 on TiO_2 in IL showed a faster production of N719 cations with a weight of the fast process A_1 as high as 90%, indicating that charge separation in the co-sensitized system is even increased by ultrafast hole trapping/transfer. As ionic liquid electrolyte is successfully regenerating the sensitizers, as long term photovoltaic stability measurements indicates (see below), the differences observed between electrodes on air and on ionic liquid could be attributed to the dynamics of hole trapping/transfer induced by the electrolyte.

Constant rates obtained for single sensitized electrodes were in the range of those previously reported in the literature for TiO_2-CdSe[33, 50] and TiO_2-N719.[47-49] It was appreciated that τ_1 and τ_2 decrease significantly in the co-sensitized electrodes, see Table 1. The beneficial effect of the synergistic action of QD-dye systems could be observed comparing with single dye or QD sensitized films. This effect could be explained as the attached dye contribution to the QD ground state regeneration leading to an improvement of electron-hole separation, a suppression of back reaction and an enhancement in electron injection rates, Fig. 2. These results suggest the dye regeneration action affecting the QD injection rate, since the hole is quickly removed from the QD the photoexcited electron does not recombine before being injected. The results obtained in this work explain the previous results on surface photovoltage[15, 19] (SPV) or on photoluminescence[16] (PL) for co-sensitized electrode. The net improvement of the amount of photoinjected electrons into TiO_2, observed by SPV, or the PL quenching for co-sensitized electrodes was due to an improvement of charge separation efficiency that avoids the charge recombination before injection.

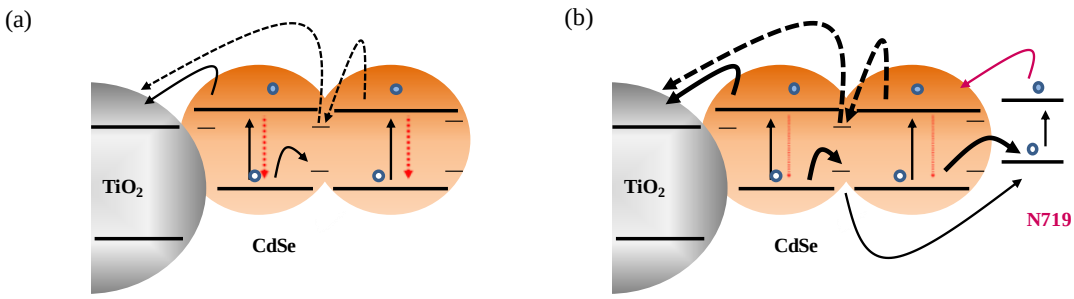

FIG. 2. Schematic diagram of dynamics of photogenerated carriers in CdSe (a) and CdSe-N719 (b) sensitized photoanodes. Solid and dashed arrows represents processes associated with a fast decay (τ_1) and a slow decay (τ_2), respectively. The arrow thickness is correlated with the strength of the process. The ultrafast trapping/transfer of holes with N719 co-sensitization increases the amount of photoinjected electrons into TiO_2.

In view of this significant effect, the photovoltaic parameters in the regenerative liquid cell configuration were evaluated. The sensitized electrodes (single and co-sensitized) were assembled with a thermally platinized TCO counter-electrode. IL redox electrolyte, 1-butyl-3-methylimidazoliumsulfide/polysulfide diluted ((w/v)=1:2) in

valeronitrile:acetonitrile mixture (v/v=1:1),[26] was introduced through a hole drilled in the counter electrode and sealed afterwards. It is important to remark that this IL electrolyte was found to be effective in regenerating both sensitizers, as well as in hole transport without corrosion problems. In this sense, sulfide/polysulfide based ILs[26] appear as a promising alternative to well established electrolytes such as cobalt or iron complexes.

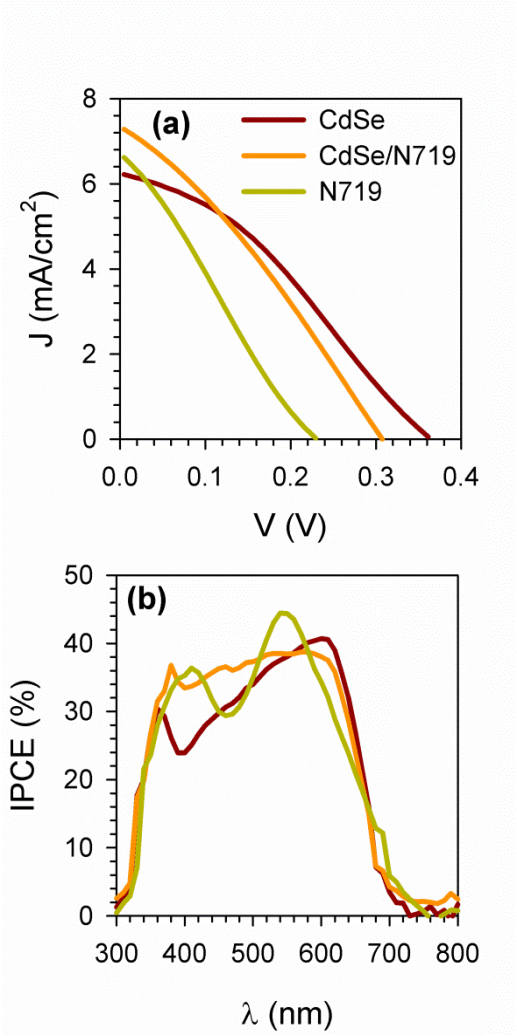

FIG. 3. Photovoltaic performance of the co-sensitized solar cells compared to single sensitized devices. (a) J-V curve and (b) IPCE.

Fig. 3(a) shows the J-V curves of the assembled solar cells and Fig. 3(b) the IPCE spectra for hybrid structures and single sensitized devices. Table 2 shows the cell performance parameters. As observed, after dye attachment the short-circuit current, J_{sc}, was boosted by 15% in the case of the hybrid sample. This result is in good agreement

with the increase of photocurrent in co-sensitized systems expected from the ultrafast measurements and discussed in Fig. 2. The effect arises from the ultrafast regeneration of the photoexcited QD by the dye. In the IPCE spectra of CdSe/N719 co-sensitized sample the contribution of both sensitizers in the photocurrent was manifested. Co-sensitized sample showed an improvement of IPCE in the wavelength range of ~350-500 nm in comparison with CdSe sensitized electrode, see Fig. 3(b). In this region, N719 sensitized electrode presents an IPCE peak. These results indicate that both sensitizers are contributing to the photocurrent as it is schematically analyzed in Fig. 2(b).

Table 2. Photovoltaic parameters of the analyzed sensitized solar cells under 1 sun illumination (AM 1.5 G)

QDSCs	$J_{sc}(mA/cm^2)$	$V_{oc}(V)$	*FF*	η *(%)*
CdSe	6.23	0.36	0.34	0.76
CdSe/N719	7.28	0.31	0.31	0.68
N719	6.62	0.23	0.26	0.49

Despites the higher J_{sc} obtained for the co-sensitized solar cell, the conversion efficiency remains lower compared to the case of single CdSe sensitized cell, which was attributed to the lower photovoltage obtained in the presence of the dye, see Table 2. In order to further understand the photovoltaic performance of the tested solar cells, impedance spectroscopy characterization was carried out. IS technique allows separation of different parts of the solar cells enabling consequently the study of sensitized electrode independently of other factors, e.g., series resistance and counter-electrode, but in the solar cell working conditions.[51] The obtained IS spectra were fitted using the previously developed models for dye and QD sensitized solar cells.[29, 51]

Chemical capacitance, C_μ, was extracted from IS data using the equivalent circuit showed in Fig. 4(a),[29, 52] and is plotted against voltage drop at the sensitized electrode, V_F, Fig. 4(b). V_F is obtained by subtracting the voltage drop at series resistance, V_s, and at counter electrode, $V_{counter}$, from the applied voltage, V_{app}, as $V_F=V_{app}-V_s-V_{counter}$. Since

C_μ records the density of states in the TiO_2, the shift of C_μ towars higher potential observed for N719 sensitized cell indicates a upward displacement of the TiO_2 conduction band (CB).[51] This shift could be explained considering that QD acts as a blocking layer preventing the direct contact of TiO_2 with the electrolyte and reducing the pH effect on the oxide surface.[29, 53] Generally, an upwards shift of TiO_2 CB produces an increase in open circuit voltage, V_{oc}, due to higher value of the splitting between the TiO_2 Fermi level and the redox position. However this behavior is not consistent with the trend observed, see Table 2, for single N719 and CdSe sensitized cells. Indeed higher V_{oc} values for QD than for N719 were observed. It can be related to the essential role of recombination resistance, R_{rec}, on V_{oc}, where higher recombination reduces V_{oc}.[53-55] As R_{rec} depends on the Fermi level position, to remove the effect of TiO_2 conduction band position, the C_μ of the different samples were shifted until they overlapped, see Fig. 4(c). Fig. 4(c) shows the C_μ vs. V_{ecb}, the voltage with respect to an equivalent common electrode in which the band shift was removed.[51] Fig. 4(d) depicts R_{rec} vs. V_{ecb}, where the same voltage shift applied to C_μ in the Fig. 4(c) was applied to the voltage in order to compare the recombination without the effect of CB shift. It can be observed that the N719 sample exhibited a value of R_{rec} significantly lower compared to CdSe sensitized cell. This fact explains the lower V_{oc} observed for N719 cell in comparison with CdSe sensitized cell, in spite of the upwards shift of TiO_2 CB for the dye sensitization.

In the case of co-sensitized cell there is no CB shift with respect to CdSe sensitized cell, see Fig. 4(b). Thus the increase in J_{sc} is associated with a direct effect of higher electron injection in the co-sensitized sample and not to a higher injection driving force, as it was discussed in Fig. 2(b). Concerning the recombination process, the co-sensitized cell presents an intermediate R_{rec} between N719 and CdSe sensitized samples and consequently the V_{oc} obtained for these samples is between the V_{oc} of the single sensitized cells, see Table 2 and Fig. 3(a). From the point of view of recombination the sample with the N719 dye showed a much higher recombination with the IL than CdSe QDs. When N719 is separated from the TiO_2 surface by an intermediate QD layer (co-sensitized sample) the recombination rate decreases (R_{rec} increases). However, the mere presence of N719 always increases the recombination rate in comparison with cells without N719. Imidazolium sulfide/polysulfide based IL has allowed us to prepare cells

with both sensitizers, N719 and CdSe QD, but the high recombination with this electrode affects deleteriously the final cell efficiency. Despites this limited efficiency, the analyzed system enables to highlight the potentiality of co-sensitized system that could significantly increase the solar cell efficiency in an optimized electrolyte where both sensitizers are stable and exhibit low recombination.

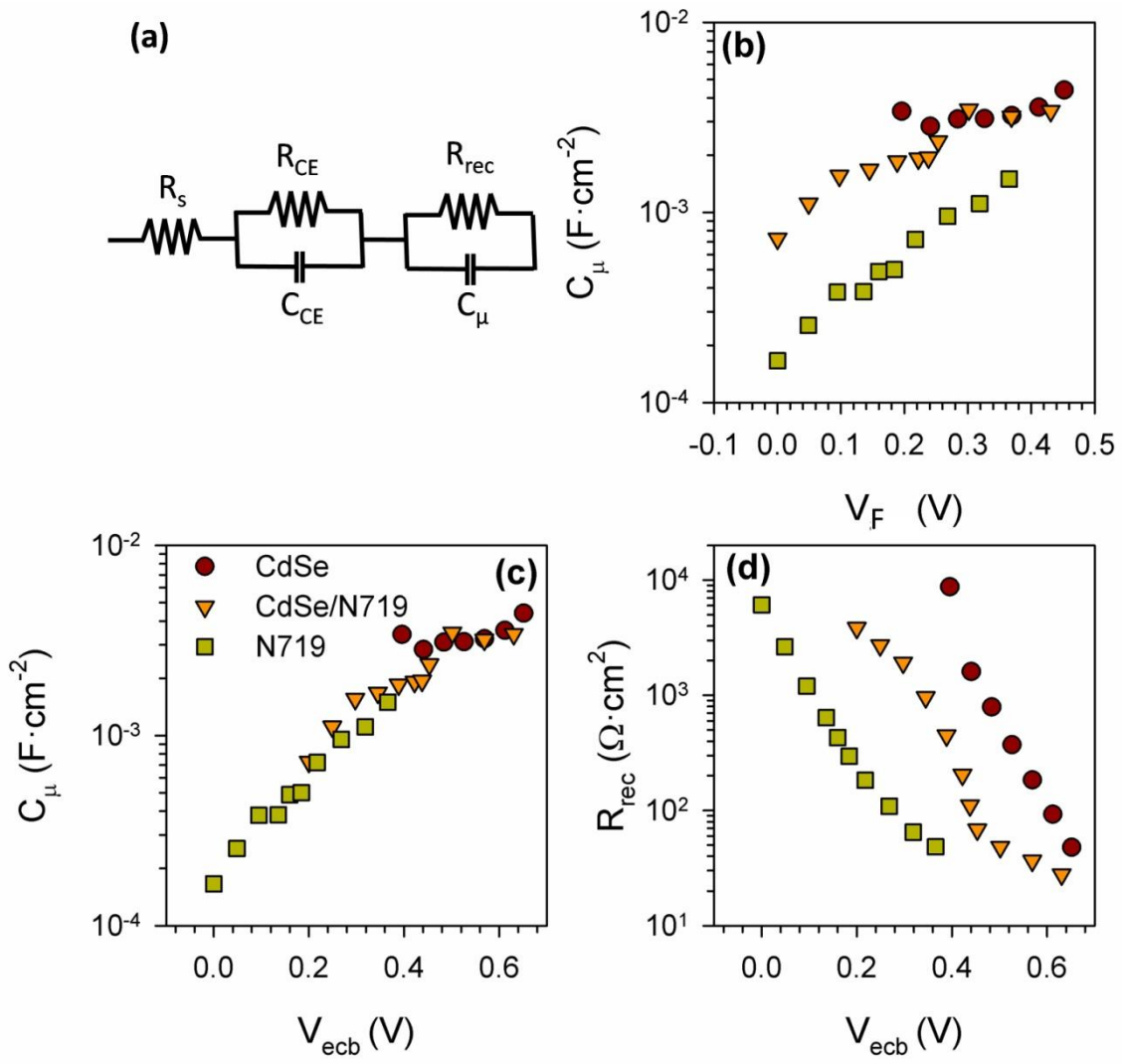

FIG. 4. Impedance spectroscopy characterization. (a) Equivalent circuit used for IS fitting. R_s is the series resistance, R_{CE} and C_{CE} are the charge transfer resistance at the counter electrode and the capacitance in the electrolyte/counterelectrode interface, respectively. R_{rec} and C_μ are the recombination resistance and the chemical capacitance, respectively, (b) Chemical capacitance, C_μ, as a function of V_F (c) and V_{ecb}, and (d) the recombination resistance as a function of V_{ecb}.

Finally, one of the most striking properties of ionic liquids for the preparation of sensitized solar cells is the higher long term stability. As it is shown in Fig. 5 the

CdSe/N719 cell retains 99% stability within one week, where the J_{sc} reduction is compensated by V_{oc} and FF increase. Cell efficiency drops 20% after 21 days, as the decrease of photocurrent cannot be further compensated by V_{oc} and FF due to their gradual decrease. These results, show a remarkable enhancement when compared with conventional aqueous polysulfide electrolytes. It is worth to mention that sulfide/polysulfides are known to slowly react with water forming sulfur-oxo species, i.e. SO_3^{2-} and SO_4^{2-},[56] and therefore gradually lowering the concentration of redox species required for operation of QDSC. The absence of these parasitic reactions, together with blocking of QD corrosion, might be the main origin of the enhancement of device stability. ILs may thus be an excellent alternative for long life QDSCs, and the efficiencies can be significantly enhanced if the recombination rate is reduced. Additionally to the formulation of less viscous electrolytes, by mixing ionic liquids with organic solvents[26] and further molecular engineering routes are under current research to synthesize sulfide/polysulfide ionic liquids with cations specially designed for slow down the recombination dynamics.

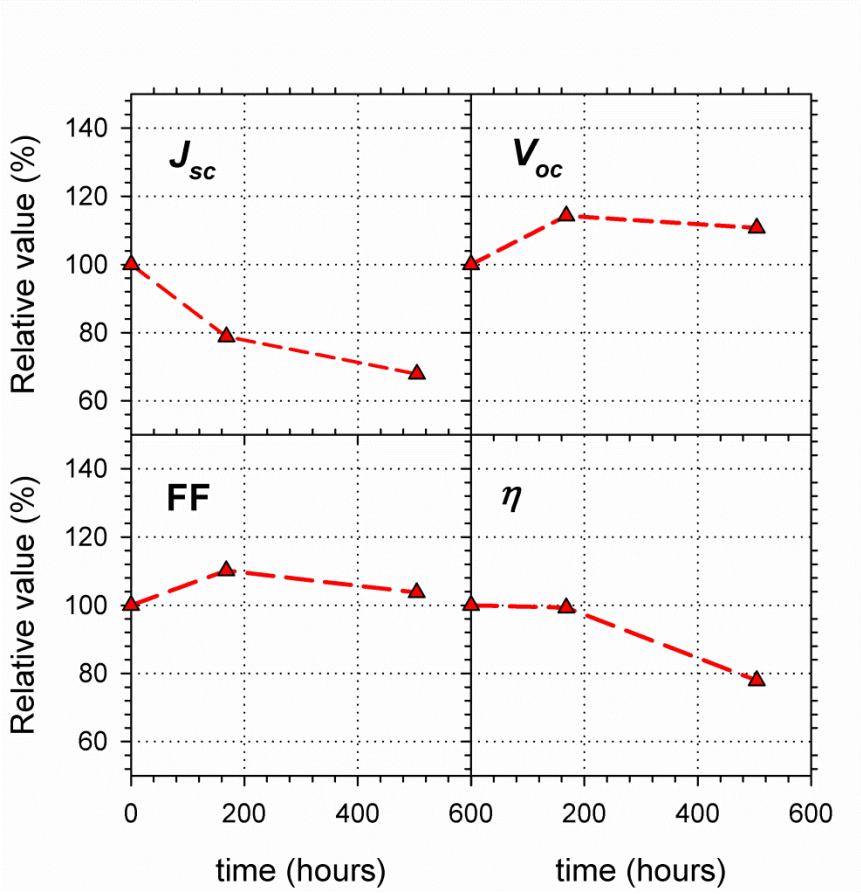

Fig. 5: Evolution of the co-sensitized solar cell parameters over time short-circuit

current, J_{sc}, open-circuit voltage, V_{oc}, Fill factor, FF, and conversion efficiency, η. Samples were stored in the dark between measurements.

Conclusions

The single and co-sensitized QD/dye solar cells highlight the potentiality of hybrid co-sensitization in sensitized solar cells. Co-sensitized samples showed enhanced photocurrent by extending the light absorption range. Additionally, there is a clear increase of photoinjection as a consequence of a decrease of the internal recombination (electron-hole recombination in the QD before electron injection) by fast trapping/transfer of holes in the presence of dye, as it has been observed here by ultrafast TG characterization. To take full advantage of co-sensitization the hole conductor material needs to fulfill the following properties, (among others not studied in this work): i) to be an stable media for both (QD and dye) light absorbers, producing long life cells and ii) to reduce as much as possible the deleterious recombination process. The 1-butyl-3-methylimidazolium sulfide/polysulfide-redox IL meets the first condition but not the second one, as it was deduced from our IS study. However, the findings reported in the present study clearly highlight the huge potential of co-sensitization that can lead to new supracollector systems with a synergetic enhancement of the light collecting properties.

Acknowledgement

This work was supported by the Institute of Nanotechnologies for Clean Energies (INCE), funded by the Generalitat Valenciana under Project ISIC/2012/008. This work was partially supported the European Union under Project ORION CP-IP 229036-2, the Ministerio de Educación y Ciencia of Spain under Projects HOPE CSD2007-00007 (Consolider-Ingenio 2010) and JES-NANOSOLAR PLE2009-0042,and the Generalitat Valenciana under Project PROMETEO/2009/058. SG and R.T.-Z. acknowledge support by MINECO of Spain under the Ramon y Cajal program. Q.S. would like to thank the PRESTO program of Japan Science and Technology Agency (JST). FP7-MC-IEF and Slovene Research Agency funding is gratefully acknowledged.

TOC Graph

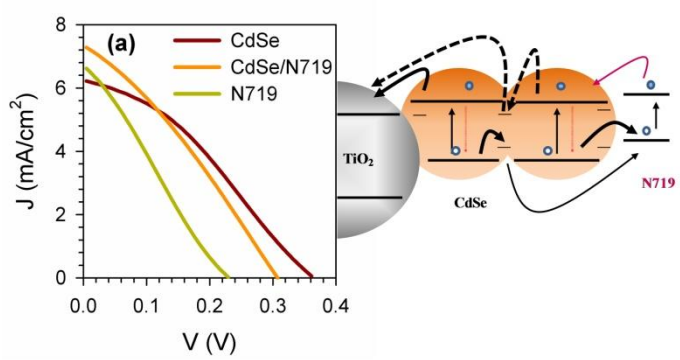

References

1. G. Hodes, *The Journal of Physical Chemistry C*, 2008, **112**, 17778-17787.
2. S. Rühle, M. Shalom and A. Zaban, *ChemPhysChem*, **11**, 2290-2304.
3. I. Mora-Seró and J . Bisquert, *The Journal of Physical Chemistry Letters*, 2010, **1**, 3046-3052.
4. P. V. Kamat, K. Tvrdy, D. R. Baker and J. G. Radich, *Chem. Rev.*, 2010, **110**, 6664–6688.
5. I. Robel, M. Kuno and P. V. Kamat, *J. Am. Chem. Soc.*, 2007, **129**, 4136-4137.
6. R. J. Ellingson, M. C. Beard, J. C. Johnson, P. Yu, O. I. Micic, A. J. Nozik, A. Shabaev and A. L. Efros, *Nano Letters*, 2005, **5**, 865-871.
7. R. D. Schaller and V. I. Klimov, *Physical Review Letters*, 2004, **92**, 186601.
8. J. B. Sambur, T. Novet and B. A. Parkinson, *Science*, **330**, 63-66.
9. O. E. Semonin, J. M. Luther, S. Choi, H.-Y. Chen, J. Gao, A. J. Nozik and M. C. Beard, *Science*, 2011, **334**, 1530-1533.

10. A. Braga, S. Giménez, I. Concina, A. Vomiero and I. Mora-Seró, *J. Phys. Chem. Lett.*, 2011, **2**, 454–460.

11. A. Kongkanand, K. Tvrdy, K. Takechi, M. Kuno and P. V. Kamat, *J. Am. Chem. Soc.*, 2008, **130**, 4007-4015.

12. S. Buhbut, S. Itzhakov, E. Tauber, M. Shalom, I. Hod, T. Geiger, Y. Garini, D. Oron and A. Zaban, *ACSNano*, 2010, **4**, 1293–1298.

13. H. J. Lee, D. W. Chang, S.-M. Park, S. M. Zakeeruddin, M. Gratzel and M. K. Nazeeruddin, *Chem. Comm.*, 2010, **46**, 8788-8790.

14. Y. Liu and J. Wang, *Thin Solid Films*, 2010, **518**, e54-e56.

15. I. Mora-Seró, D. Gross, T. Mittereder, A. A. Lutich, A. S. Susha, T. Dittrich, A. Belaidi, R. Caballero, F. Langa, J. Bisquert and A. L. Rogach, *Small*, 2010, **6**, 221-225.

16. I. Mora-Seró, V. Likodimos, S. Giménez, E. Martínez-Ferrero, J. Albero, E. Palomares, A. G. Kontos, P. Falaras and J. Bisquert, *The Journal of Physical Chemistry C*, 2010, **114**, 6755-6761.

17. M. Shalom, J. Albero, Z. Tachan, E. Martínez-Ferrero, A. Zaban and E. Palomares, *J. Phys. Chem. Lett.*, 2010, **1**, 1134–1138.

18. H. Choi, R. Nicolaescu, S. Paek, J. Ko and P. V. Kamat, *ACS Nano*, 2011, **5**, 9238–9245.

19. I. Mora-Seró, T. Dittrich, A. S. Susha, A. L. Rogach and J. Bisquert, *Thin Solid Films*, 2008, **516**, 6994–6998.

20. S. Gimenez, A. L. Rogach, A. A. Lutich, D. Gross, A. Poeschl, A. S. Susha, I. Mora-Sero, T. Lana-Villarreal and J. Bisquert, *J. Appl. Phys.*, 2011, **110**.

21. A. Zaban, O. I. Micic, B. A. Gregg and A. J. Nozik, *Langmuir*, 1998, **14**, 3153-3156.

22. M. Shalom, S. Dor, S. Rühle, L. Grinis and A. Zaban, *The Journal of Physical Chemistry C*, 2009, **113**, 3895-3898.

23. P. K. Santra and P. V. Kamat, *J. Am. Chem. Soc.*, 2012, **134**, 2508-2511.

24. R. Tena-Zaera, A. Katty, S. Bastide and C. Lévy-Clément, *Chemistry of Materials*, 2007, **19**, 1626-1632.

25. H. J. Lee, D. W. Chang, S.-M. Park, S. M. Zakeeruddin, M. Gratzel and M. K. Nazeeruddin, *Chemical Communications*, **46**, 8788-8790.

26. V. Jovanovski, V. González-Pedro, S. Giménez, E. Azaceta, G. Cabañero, H. Grande, R. Tena-Zaera, I. Mora-Seró and J. Bisquert, *J. Am. Chem. Soc.*, 2011, **133**, 20156-20159.

27. Q. Shen, D. Arae and T. Toyoda, *Journal of Photochemistry and Photobiology A: Chemistry*, 2004, **164**, 75-80.

28. Q. Shen and T. Toyoda, *Thin Solid Films*, 2003, **438–439**, 167-170.

29. V. Gonzalez-Pedro, X. Q. Xu, I. Mora-Sero and J. Bisquert, *Acs Nano*, 2010, **4**, 5783-5790.

30. H. Lee, M. Wang, P. Chen, D. R. Gamelin, S. M. Zakeeruddin, M. Grätzel and M. K. Nazeeruddin, *Nano Letters*, 2009, **9**, 4221-4227.

31. Jovanovski, V.; Marcilla, R.; Mecerreyes, D.; Cabanero, G.; Tena-Zaera, R.; Mora-Seró, I. Bisquert, J. Eur. Pat. No. 10382132.8-2119 and PCT/EP/2011/058143, 2010

32. L. J. Diguna, Q. Shen, A. Sato, K. Katayama, T. Sawada and T. Toyoda, *Materials Science and Engineering: C*, 2007, **27**, 1514-1520.

33. N. s. Guijarro, T. Lana-Villarreal, Q. Shen, T. Toyoda and R . Gómez, *The Journal of Physical Chemistry C*, 2010, **114**, 21928-21937.

34. N. s. Guijarro, Q. Shen, S. Giménez, I. n. Mora-Seró, J. Bisquert, T. Lana-Villarreal, T. Toyoda and R . Gómez, *The Journal of Physical Chemistry C*, 2010, **114**, 22352-22360.

35. Q. Shen, K. Katayama, T. Sawada and T. Toyoda, *Thin Solid Films*, 2008, **516**, 5927-5930.

36. Q. Shen, K. Katayama, T. Sawada, M. Yamaguchi, Y. Kumagai and T. Toyoda, *Chemical Physics Letters*, 2006, **419**, 464-468.

37. Q. Shen, K. Katayama, M. Yamaguchi, T. Sawada and T. Toyoda, *Thin Solid Films*, 2005, **486**, 15-19.

38. J. Kim, C. Meuer, D. Bimberg and G. Eisenstein, *Applied Physics Letters*, 2009, **94**.

39. K. Katayama, M. Yamaguchi and T. Sawada, *Applied Physics Letters*, 2003, **82**, 2772-2774.

40. Q. Shen, M. Yanai, K. Katayama, T. Sawada and T. Toyoda, *Chemical Physics Letters*, 2007, **442**, 89-96.

41. J. J. Kasinski, L. A. Gomez-Jahn, K. J. Faran, S. M. Gracewski and R. J. D. Miller, *The Journal of Chemical Physics*, 1989, **90**, 1253-1269.

42. Y.-l. Yan, Y. Li, X.-f. Qian, J. Yin and Z.-k. Zhu, *Materials Science and Engineering: B*, 2003, **103**, 202-206.

43. M. Samadpour, S. Giménez, P. P. Boix, Q. Shen, M. E. Calvo, N. Taghavinia, A. I. zad, T. Toyoda, H. Míguez and I. Mora-Seró, *Electrochimica Acta*, 2012, **75**, 139-147.

44. K. Tvrdy and P. V. Kamat, *The Journal of Physical Chemistry A*, 2009, **113**, 3765-3772.

45. Q. Shen, Y. Ayuzawa, K. Katayama, T. Sawada and T. Toyoda, *Applied Physics Letters*, 2010, **97**, 263113-263113.

46. L. Min and R. J. D. Miller, *Applied Physics Letters*, 1990, **56**, 524-526.

47. Q. Shen, Y. Ogomi, B.-w. Park, T. Inoue, S. S. Pandey, A. Miyamoto, S. Fujita, K. Katayama, T. Toyoda and S. Hayase, *Physical Chemistry Chemical Physics*, 2012, **14**, 4605-4613.

48. N. A. Anderson and T. Lian, *Annual Review of Physical Chemistry*, 2004, **56**, 491-519.

49. S. E. Koops, B. C. O'Regan, P. R. F. Barnes and J. R. Durrant, *J. Am. Chem. Soc.*, 2009, **131**, 4808-4818.

50. V. I. Klimov, D. W. McBranch, C. A. Leatherdale and M. G. Bawendi, *Physical Review B*, 1999, **60**, 13740-13749.

51. F. Fabregat-Santiago, G. Garcia-Belmonte, I. Mora-Sero and J. Bisquert, *Phys. Chem. Chem. Phys.*, 2011, **13**, 9083-9118.

52. I. Mora-Seró, S. Giménez, F. Fabregat-Santiago, R. Gómez, Q. Shen, T. Toyoda and J. Bisquert, *Accounts of Chemical Research*, 2009, **42**, 1848-1857.

53. E. M. Barea, M. Shalom, S. Gimenez, I. Hod, I. Mora-Sero, A. Zaban and J. Bisquert, *J. Am. Chem. Soc.*, **132**, 6834-6839.

54. T. Marinado, K. Nonomura, J. Nissfolk, M. K. Karlsson, D. P. Hagberg, L. Sun, S. Mori and A. Hagfeldt, *Langmuir*, 2009, **26**, 2592-2598.

55. F. Fabregat-Santiago, J. Bisquert, G. Garcia-Belmonte, G. Boschloo and A. Hagfeldt, *Solar Energy Materials and Solar Cells*, 2005, **87**, 117-131.

56. W. E. Kleinjan, A. d. Keizer and A. J. H. Janssen, *Water Research*, 2005, **39**, 4093-4100.